ESTIMATION OF ABSORBED PHOTOLYTIC DOSAGE AND QUANTUM YIELD USING UV-VIS AND FTIR SPECTROSCOPIES

by

J.W. Martin, T. Nguyen, E. Byrd and N. Embree
Building and Fire Research Laboratory
National Institute of Standards and Technology
Gaithersburg, MD 20899 USA

Reprinted from the American Chemical Society, PSME. Proceedings. Vol. 82, Spring Meeting, March 26-30, 2000, San Franicso, CA, 2000.

NIST
National Institute of Standards and Technology
Technology Administration, U.S. Department of Commerce

American Chemical Society, PSME, Vol. 82, March, 2000

ESTIMATION OF ABSORBED PHOTOLYTIC DOSAGE AND QUANTUM YIELD USING UV-VIS AND FTIR SPECTROSCOPIES

J.W. Martin, T. Nguyen, E. Byrd, and N. Embree

National Institute of Standards and Technology, Gaithersburg, MD 20899

Introduction

This report forms part of a large study that has been designed around an effective dosage model that has gained widespread acceptance in the medical and biological fields (1). The effective dosage model, which relates damage to the energy of radiation absorbed in the material through the quantum yield, has a firm basis in the principles of photochemistry. Use of effective UV-visible radiation dosage accounts for all spectral UV-visible radiation that impinges on, is absorbed by, and photolytically degrades a material. Thus, the effective dosage model can be modified to account for the effects of environmental conditions such as relative humidity, temperature, and radiant flux, on the degradation.

The effective dosage model has the form (2):

$$D_{eff}(t) = \int_0^t \int_{\lambda_{min}}^{\lambda_{max}} E_c\left(\lambda_{uv}, t\right)\left(1 - 10^{-A\left(\lambda_{uv}, t\right)}\right)\phi(\lambda)\, d\lambda\, dt$$

where D_{eff} (t) is the effective dosage at time t; λ_{min} and λ_{max} are the minimum and maximum photolytically effective UV-visible wavelengths; $A(\lambda_{uv},t)$ is the absorption of the sample at a specified wavelength in the UV-visible region and at time t; $E_c(\lambda_{uv},t)$ is the irradiance to which the coating is exposed to at time t; and $\phi(\lambda_{uv})$ is the apparent quantum yield of the coating at a particular wavelength. Damage, D_{dam}, is related to photolytic dosage through the quantum yield:

$$D_{dam} = \phi(\lambda_{uv}) \cdot D_{dos}(\lambda_{uv})$$

where D_{dos} is the absorbed dosage (defined as the fraction of incident radiation absorbed by the material). D_{dos} is the product of E_c (λ_{uv},t) and A (λ_{uv},t), both of which were obtained experimentally in this study using UV-visible spectroscopy. The damage was measured using FTIR transmission spectroscopy by monitoring coating degradation as a function of time or absorbed dosage. The apparent quantum yield was estimated by taking the initial slope of the damage vs absorbed dosage curve. A computer program has been written to estimate absorbed dosage, damage, and quantum yield using inputs provided by UV-visible and FTIR measurements.

Experimental

A model thermoset acrylic melamine coating consisting of a mixture of a hydroxy-terminated acrylic polymer and a partially-alkylated amine crosslinking agent was used. The ratio of acrylic resin to melamine crosslinking agent was, by mass, 70:30. Coatings were applied to CaF_2 substrates by spin coating followed by curing at 130 °C for 20 minutes. All coated samples were well cured, and coating thickness, which was 10 μ m ± 2 μ m, was uniform within approximately 97% for the entire coated surface.

Figure 1 displays the experimental setup used in this study. Complete details on the exposure cells, UV light source (i.e., solar simulator, narrow bandwidth filters and their characteristics, etc.), instrumentation, and controlled systems are described elsewhere (3). Coated CaF_2 samples were placed in an exposure cell, which consisted of 12 windows corresponding to the 12 exposure conditions. Ten of the windows contained narrow bandwidth filters covering radiation from 290 nm to 525 nm, one was completely covered, and one was left open without a filter (designated as "full UV"). A quartz disk was placed directly underneath the filter and above the coated CaF_2 plate. Each cell contained an inlet and an outlet to allow air with the desired temperature and relative humidity (RH) to circulate in the space between the quartz disc and the coated CaF_2 plate. Temperature and humidity sensors connected to each cell and to a computer were used to control temperature and RH in each cell.

To test the validity of the effective dosage model, specimens were exposed to a combination of over 200 different conditions of temperature, RH and UV-visible radiation. Nominal RHs were <<1% (dry), 20%, 40%, 70% and 90% at nominal temperatures of 30 °C, 40 °C, 50 °C and 60 °C for 12 different UV conditions. The RH in each cell was provided by a specially-designed humidity generator, which controlled RHs in the 0% - 90% range to within ±3% by controlling the ratio of dry air and moisture-saturated air. The temperature in each cell was maintained within ± 2°C of the desired value. The radiation source was supplied by two 1000 W xenon arc solar simulators, which provided infrared-free, near ambient temperature (24 °C) radiation with wavelengths between 275 nm and 800nm.

At specified time intervals, a UV-visible spectrometer equipped with a fiber-optics sensor and connected to a robotic controlling system was used to measure the irradiance at each of the 12 windows. These measurements were made in the absence of the exposure cells. At the same time, transmittance spectra of the filters and the quartz plates were collected using a UV-visible spectrometer equipped with an automated sampling system. The measurements of the irradiance and the transmittance of the filters and the quartz plates at each window as a function of exposure time were used to calculate the total radiation impinging on the coatings.

UV-visible and IR absorbance spectra of the coating as a function of exposure were recorded by UV-visible and FTIR spectrometers using an automated sampling accessory. This automated sampling system allowed unattended, efficient, and quick recording of the UV and IR absorbance spectra of the coating specimens at all 12 windows. At each specified time interval, the coated CaF_2 plate was removed from the exposure cell, fitted into a demountable ring on the automated sampling device, and UV and IR spectra were collected. UV-visible spectra were recorded from 190 nm to 820 nm with a resolution of 1 nm at 2s per scan. These data were employed to calculate the radiation absorbed in the coating and also to monitor coating changes with exposure. FTIR spectra were the average of 128 scans that were recorded at a resolution of 4 cm^{-1} using a liquid nitrogen-cooled MCT detector and dry air as the purge gas.

The apparent quantum yield in this study is expressed as the change in FTIR intensity per unit thickness per amount of radiation absorbed in the coating. If FTIR intensity for the degradation is expressed in an absorbance unit (A), with thickness in meter (m), and radiation absorbed by the coating in Joules (J), the apparent quantum yield is expressed in A m^{-1} J^{-1}.

Results and discussion

Figure 2 shows representative FTIR difference spectra (spectrum of exposed specimen-spectrum of specimen before exposure) of the acrylic melamine coatings after exposure for 2040 h under different UV conditions and at 50 °C/<<1% RH. Decreases in FTIR intensity were observed in the 2750 cm^{-1}-3050 cm^{-1} and 1600-1000 cm^{-1} regions and increases in intensity occurred in the 3100 cm^{-1}-3400 cm^{-1} region. Several new bands appeared, including those at 1760 cm^{-1}, 1670 cm^{-1}, 1630 cm^{-1}, and 1420 cm^{-1}. In all cases, the degradation for each of the ten filters was much less than that under "full UV". In addition, the coating also underwent changes even in the absence of light and in very dry conditions (<<1% RH), as evidenced by decreases of FTIR intensities in various bands in the 3000-2850 cm^{-1} and 1000-1600 cm^{-1} regions. Changes in the coatings under very dry/no UV light conditions were probably due to dark hydrolysis. The water required for the hydrolysis reactions was presumably produced by a number of reactions that might take place during curing or post curing (4).

In this study, the amide C=O band at 1670 cm^{-1} and the C-O band at 1085 cm^{-1} were used to follow oxidation and chain scission, respectively. In Figure 3, typical oxidation and chain scission (in IR absorbance) are presented as a function of photolytic dosage for specimens exposed under different UV conditions at 50°C/<<1%RH. As in the case of damage/time relation (3), both oxidation and chain scission processes in photolysis by the full UV condition (insert) were an order of magnitude greater than those at any particular narrow bandwidth filter. In the presence of moisture, both the chain scission and oxidation were substantially greater than those exposed to dry conditions, due to both hydrolysis and moisture-enhanced photolysis occurring in this coating. Further, both the extent and rate of degradation increased with increased RH (3). Because of the experimental design for this study, the effects of each of these processes, i.e., post curing, hydrolysis, moisture-enhanced photolysis, and photolysis, on the photodegradation of acrylic melamine coatings have been individually separated and quantified.

The apparent quantum yield was determined from the initial portion of the slope of the damage/dosage curve to avoid complications from multiple degradation processes. The damage/dosage relationship has been fitted

using a fourth-order polynomial function to provide the quantum yield. Because the damage/dosage relationship was not linear, the apparent quantum yield decreased with dosage, presumably due to increased shielding of the coating by degradation products and/or decreased availability of weak links. Typical apparent quantum yields for the chain scission and oxidation of samples exposed to 50 °C/<<1% RH condition under full UV and several narrow bandwidth filters are given in Table 1.

Table 1. Quantum yields of the oxidation and chain scission of acrylic-melamine coatings exposed at 50 °C/<<1% RH and under different UV conditions

	Apparent Quantum Yield[a], $x10^{-6}$ $Am^{-1}J^{-1}$			
	Full UV	312 nm[b] (3.7 nm)[c]	354 nm[b] (26.2 nm)	450 nm[b] (135.3 nm)
Oxidation	0.30± 0.03	3.1 ± 2.2[d]	0.80± 0.2	0.30± 0.04
Chain Scission	0.22±0.02	1.6± 1.3	0.60± 0.2	0.20± 0.05

[a]Average of four measurements; [b]This number indicates the center wavelength of each filter; [c]Number in the parenthesis indicates the full width half maximum (FWHM) values of each filter; and [d]Number following the symbol ± indicates one estimated standard deviation.

The quantum yields for most of the photodegradation processes for this coating were small, as is typical for photolysis of polymers in the solid state (5). Quantum yields of polymer chain scission have been observed to be very low below the glass transition temperature (T_g) but to increase rapidly to the value obtained for the same polymer in solution as the temperature is increased to above T_g (6).

Estimates of the photolytic absorbed dosage and apparent quantum yield were found to be extremely sensitive to a number of variables, including initial UV-visible absorption of the coatings, coating degradation products, anomalous UV absorption of the substrate, spectral handling of infrared and UV-visible spectra, and the reproducibility of UV-visible and FTIR spectrometers.

Conclusions

An effective dosage model has been introduced for predicting the service life of polymeric materials exposed to UV light. The effective dosage model, which relates material damage through the apparent quantum yield, has a firm basis in the principles of photochemistry. The primary inputs into this model are photolytic absorbed dosage and damage, and the outputs are effective dosage and apparent quantum yield. Laboratory experiments were designed to provide data for these parameters over wide ranges of conditions to encompass those environments to which a coating is expected to be exposed in the field and to allow the effects of competing degradation reactions to be separated. Estimates of the absorbed dosage and apparent quantum yield were found to be very sensitive to initial UV-visible absorption of the coatings, coating degradation products, anomalous UV absorption of the substrate, spectral handling of infrared and UV-visible spectra, and the reproducibility of UV-visible and FTIR spectrometers.

References

1. M.M. Caldwell, Photophysiology, 6 (1971)131.
2. J. W. Martin, S. C. Saunders, F. L. Floyd, and J. P. Wineburg, Methodologies for Predicting the Service Life of Coatings, Federation Series on Coatings Technology, Federation of Societies for Coatings Technology, PA, 1996.
3. J.W. Martin, T. Nguyen, E. Byrd, N. Embree, and B. Dickens, Relating Laboratory and Outdoor Exposures of Acrylic Melamine Coatings: I. Estimation of Effective Photolytic Dosage and Quantum Yield, to be Submitted to Polymer Degradation and Stabilization.
4. D.R. Bauer and R.A Dickie, J. Polym. Sc., Polym. Physics Edition, 18 (1980) 1997.
5. B.Randy and J.F. Rabeck, Photodegradation, Photo-oxidation and Photostabilization of Polymers: Principles and Applications, John Wiley & Sons, New York, 1975, pp83-87.
6. E. Dan and J.E. Guillet, Macromolecules, 6 (1973) 230.

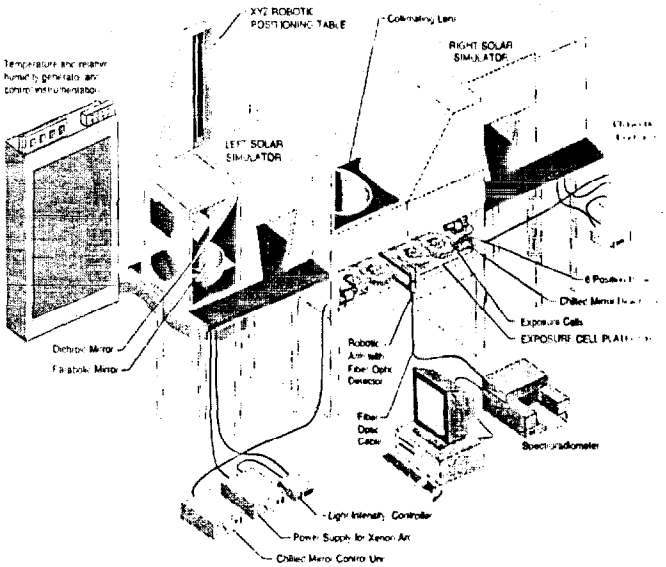

Figure 1. Experimental setup for measuring effective photolytic dosage and quantum yields of polymer coatings exposed to different UV/relative humidity/temperature conditions.

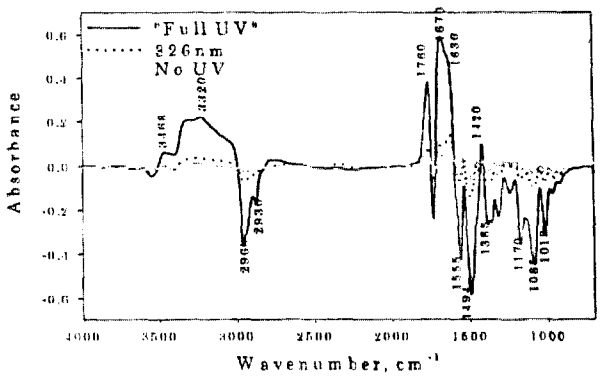

Figure 2. FTIR difference spectra for an acrylic melamine coating exposed for 2040 h to different UV conditions at 50 °C/<<1% relative humidity.

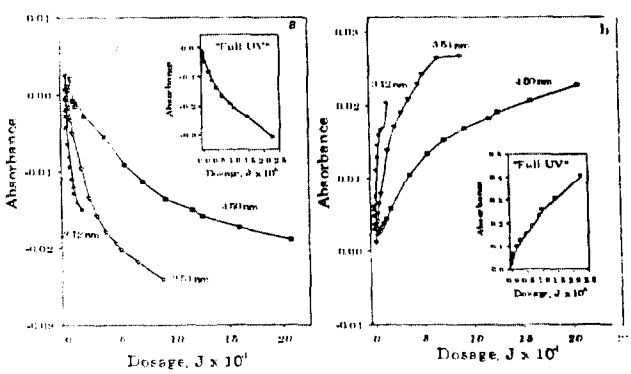

Figure 3. Oxidation (a) and chain scission (b) as a function of absorbed dosage of a acrylic melamine coating exposed to 50 °C/<<1% RH for full UV and several narrow bandwidth filters. The initial slopes of these curves are used for obtaining the apparent quantum yield.